Atmospheric
Measurement
Techniques

Open Access

EGU

Supplement of

Characterisation of a self-sustained, water-based condensation particle counter for aircraft cruising pressure level operation

Patrick Weber et al.

Correspondence to: Patrick Weber (p.weber@fz-juelich.de) and Ulrich Bundke (u.bundke@fz-juelich.de)

Electronic Adjustments for the Magic LP 210

The following supplement materials of the manuscript "Characterization of a self-sustained, water-based condensation particle counter for aircraft cruising pressure level operation" contains detailed information about the signal processing optimisation of the CPC Magic-LP 210 and the multiply charge correction.

Based on this study, Aerosol Dynamics Inc. has updated their low-pressure CPCs to operate down to 200 hPa.

Figure 1 shows an idealized signal from the optics electronics. The analogue signal is compared to the "detector threshold" (normally 250mV) which produces a digital pulse that increments a counter in the microcontroller.

The "baseline voltage", i.e., the signal with no particles present, could be above or below 0 volts due to imperfection in the optics and electronics, as shown in Figure 2. There is always some stray light that reaches the photo detector, and all operational amplifiers have some non-zero offset. To compensate, a "detector offset" is add to the analogue signal to adjust the baseline voltage to zero.

Since the stray light reaching the photodetector is proportional to the laser power, the firmware automatically adjusts both the laser power and detector offset with pressure. The specific relationship between laser power and detector offset are set at the factory and vary from instrument to instrument.

To operate the MAGIC 210-LP at pressures lower than then it was designed for, voltage offset, and detector thresholds had to be determined experimentally below 300 hPa. At 250 hPa, we found that the required laser power was so high that the electronics was incapable of zeroing out the baseline voltage. To compensate the detector threshold was increased above the factory setting of 250mV (figure 3).
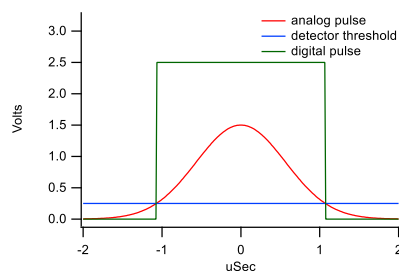
Figure S1: Ideal signal from one particle passing through the optics detector
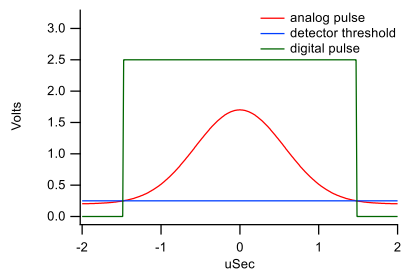

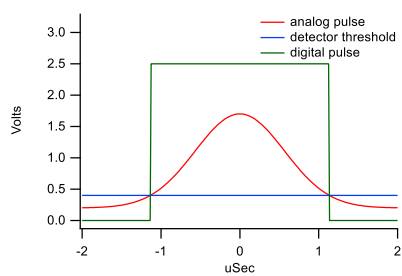Figure S2: Effect of imperfections in optics and electronics on the baseline voltage.

Figure S3: Detector threshold is increased to compensate for inability of the electronics to completely cancel out the baseline signal at lowest pressure.

As the absolute pressure during operation decreases, also the droplet growth is reduced resulting in smaller droplets, which need to be counted. This is compensated by adjusting the laser power and the detector threshold. The instrument firmware makes these adjustments automatically based on a lookup table, and the 1 Hz absolute pressure reading. Concentrations are reported with respect at laboratory conditions of 25°C and 1013 hPa.

The following optimisation step was applied. The MAGIC 210-LP was designed for operation at pressure levels as low as 300 hPa. We were able to extend the range of operation down to 200 hPa by the adjustment of the initial laser power to different pressure levels. In **Error! Reference source not found.** the counting efficiency is expressed as the number concentration measured by the MAGIC

instrument divided by the number concentration measured by the G-CPC instrument and is shown at different pressure levels for 100 nm sized particles for a range of initial laser power settings. To compensate the effect that particles grow less efficiently at lower pressures the threshold and the laser power are controlled as a function of the internal measured pressure. Here the laser power is increased, and the offset is lowered with decreasing pressure values. At 250 hPa the adjusted detector threshold reaches 0 V and only the constant parameter of the detector threshold limits the counted signals. The detector offset adjusts for non-ideal electronics and optics so that the signal without any particles present is at zero volts. The detector threshold is the voltage level that is used to determine if a particle is in the laser beam. In Figure 4 each graph was obtained from measurements at a detector threshold setpoint of 250 mV. The only exception is the "250 hPa optimised". To compensate for the increased stray light, the detector threshold was increased from 250 mV towards 400 mV. This series of measurements was conducted with the increased 400 mV detector threshold. This method of adjusting the initial laser power setting increased the secure bandwidth of laser power that could be applied, without false counts. A stable counting rate was obtained for the set point at 500 µW for all pressure ranges. For higher pressure levels, the offset must be set to a value of over 300 mV to compensate for the higher threshold of 400 mV at ground pressure levels.
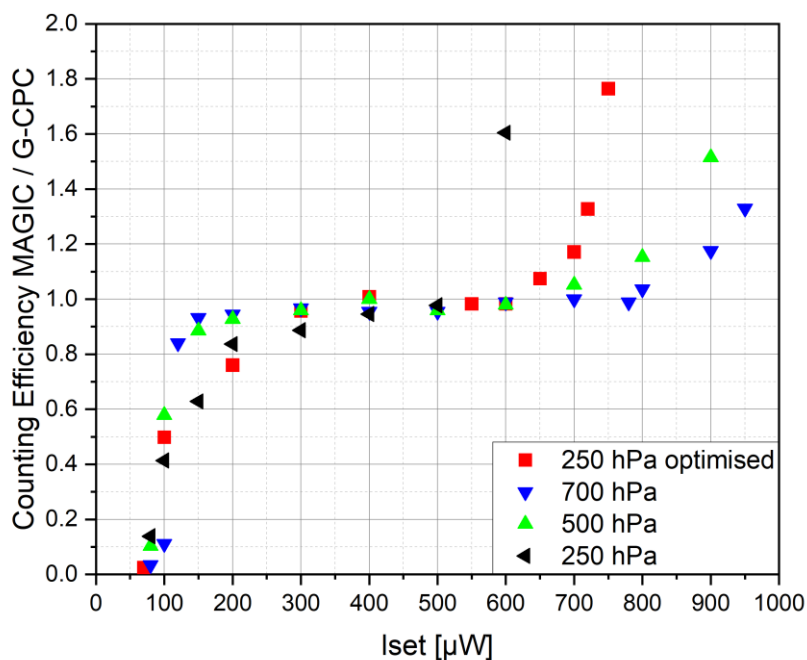

Figure S4 Counting Efficiency response for different initial laser power settings (Lset) and pressure levels for 100 nm particles.

The multi-charge correction after Bundke, (2015):

Using a diffusion charger in combination with a DMA and using FCE as reference instrument it must be considered that particles passing the DMA may carry multiple charges. If a particle exiting the DMA carries *n* charges the FCE will count these particle *n* times whereas a CPC will register just one particle. Thus, a multi-charge correction must be applied to the FCE data:

$$N_{FEC}(D_p) = \sum_{n=0}^{\infty} nN \cdot (D_p(U,n))\eta(n, D_p(U,n)) \tag{S1}$$

For technical reasons – only charged particle will pass the DMA – and as a good approximation we limit the sum to $\{1 \leq n \leq 2\}$. Thus, only single and double charged particles are considered. Here, $N^*(D_p)$ denotes the 'true' particle number per time interval as function of the electrostatic mobility particle diameter $D_p(U, n)$, U denotes the DMA voltage and $\eta(n, D_p)$ the normalised charge distribution of particles carrying *n* charges. For the latter, we use the approximation by Wiedensohler (1988):

$$\eta(n) = 10 \sum_{i=0}^{5} a_i(n) \log\left(\frac{D_p}{nm}\right) \tag{S2}$$

The approximation coefficients a_i are defined

Table S1. Approximation coefficients

	n				
$a_i(n)$	−2	−1	0	1	2
a_0	−26.3328	−2.3197	−0.0003	−2.3484	−44.4756
a_1	35.9044	0.6175	−0.1014	−0.6044	79.3772
a_2	−21.4608	0.6201	0.3073	0.48	−62.8900
a_3	7.0867	−0.1105	−0.3372	0.0013	26.4492
a_4	−1.3088	−0.1260	0.1023	−0.1544	−5.7480
a_5	0.1051	0.0297	−0.0105	0.032	0.5059

Thus, $N_{FCE(Dp)}$ joins as

$$N_{FCE}(D_p) = N \cdot \left(D_p(U, n = 1)\right)\eta\left(n = 1, D_p(U, n = 1)\right) + 2N \cdot \left(D_p(U, n = 1)\right)\eta\left(n = 2, D_p(U, n = 2)\right) \tag{S3}$$

Equivalent to equation the number concentration of N_{CPC} of the CPC is given by

$$N_{CPC}(D_p) = N \cdot \left(D_p(U, n = 1)\right)\eta\left(n = 1, D_p(U, n = 1)\right) + N \cdot \left(D_p(U, n = 1)\right)\eta\left(n = 2, D_p(U, n = 2)\right) \tag{S4}$$

Using this equation, the ratio N_{CPC}/N_{FCE} gives the correction factor $\xi(D_p)$.

For Using

$$A = N \cdot \left(D_p(U, n = 1)\right) \eta \left(n = 1, D_p(U, n = 1)\right) \tag{S5}$$

And

$$B = N \cdot \left(D_p(U, n = 2)\right) \eta \left(n = 2, D_p(U, n = 2)\right) \tag{S6}$$

ξ can be expressed as

$$\xi = \frac{N_{CPC}}{N_{FCE}} = \frac{A+B}{A+2B} = \frac{1+\frac{A}{B}}{2+\frac{A}{B}} \tag{S7}$$

Substituting the expressions of A and B in C and D giving

$$C = \frac{N \cdot \left(D_p(U, n=1)\right)}{N \cdot \left(D_p(U, n=2)\right)} \tag{S8}$$

$$D = \frac{\eta \left(n=1, D_p(U, n=1)\right)}{\eta \left(n=2, D_p(U, n=2)\right)} \tag{S9}$$

Therefore the factor C is calculated by using the size distribution measurement, Here, the diameters $D_p(U,n=1)$, $D_p(U,n=2)$, are associated with the different DMA voltages U. They are calculated by solving the implicit equation

$$D_p = \frac{neC(D_p)}{3\pi\mu} \cdot \frac{2\pi L U}{\ln\left(\frac{r_a}{r_i}\right)Q_{Sh}} \tag{S10}$$

With n as the number of charges, e as elemental charge of $1.6022*10^{-19}$C, μ as the gas viscosity, L the DMA length, r_a the DMA outer radius, r_i the DMA inner radius and Q_{sh} as the sheath flow.

The factor D is calculated using the equation by Wiedensohler (1988).

Finally, he multiple charge correction can be expressed by

$$N_{FEC}^* = \xi\left(D_p\right)N_{FCE} \tag{S11}$$

as N_{FEC}^* as the corrected electrometer number concentration and ξ as the calculated correction factor.

The following section describes the line loss calculations. The calculations were from Hinds (1999) and Baron (2001)
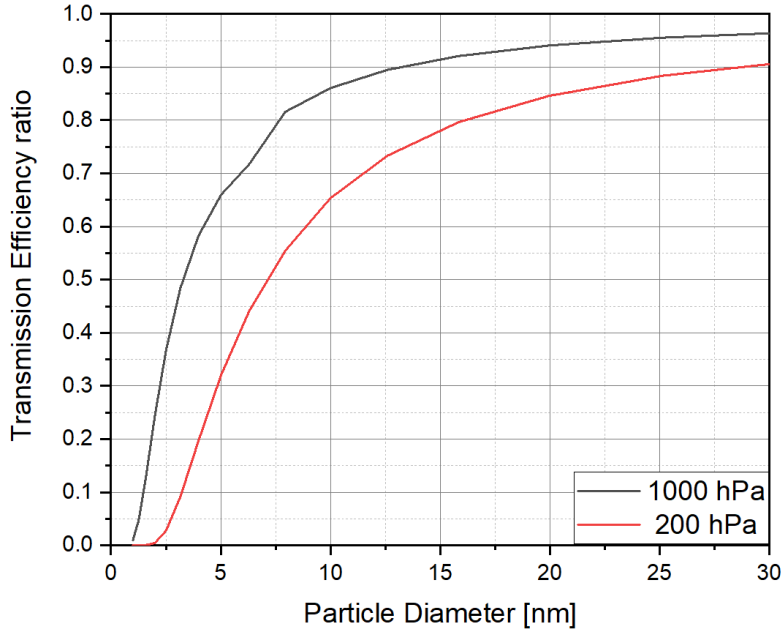
Figure S5. Particle Loss calculations for different particle diameter. The values displayed are for the final package installed at the aircraft.

Aerosol sampling is an important issue, when aerosol measurements claim to cover a total range of aerosol properties and size ranges. Particles can be lost in the sampling line by impaction, sedimentation or diffusion. For very small particles, the diffusion is the most important mechanism for particle losses. Those can be illustrated by diffusion losses in a cylindrical tube under laminar flow. The first thing to recognize is the Stokes`s Law. This fundamental force F describes the total resisting force a spherical particle experience by moving through a medium.

$$F = 3\pi\eta v d \tag{S12}$$

With η is the viscosity of the medium, v the velocity of the particle and d the diameter of the particle. The Cunningham correction Cc factor has to correct an important assumption of this force. The assumption of the Stokes`s Law is, that the relative velocity of the gas at the surface of the sphere is zero. This assumption becomes an issue for small particles at the range of the mean free path.

$$F = \frac{3\pi\eta v d}{C_c} \tag{S13}$$

The Cunningham correction factor can be calculated using the mean free path χ by

$$C_c = 1 + \frac{\chi}{d}[2.514 + 0.8 \exp\left(-0.39\frac{d}{\chi}\right)] \tag{S14}$$

Then the diffusion coefficient ξ for laminar flow can be calculated considering the temperature T by

$$\xi = \frac{1.38 \cdot 10^{-23}[\frac{J}{K}] \cdot T \cdot C_c}{3\pi\eta d} \tag{S15}$$

With this the dimensionless diffusion parameter µ can be calculated with the length of the tube l and the air flow rate f.

$$\mu = \xi \frac{l}{f} \qquad\qquad (S16)$$

Finally, the loss fraction can be described by

$$Loss = 0.819e^{-11.5\mu} + 0.0975e^{-70.1\mu} + 0.0325e^{-179\mu} \qquad\qquad (S17)$$

The final line loss is the product of two settings. Here, the main aerosol sampling line with a flow rate of 4 l/min for the final instrument package and a length of 1 meter till the splitting point, where the MAGIC-LP has a flow rate of 0.3 l/min and 30 cm distance.

Bundke, U., Berg, M., Houben, N., Ibrahim, A., Fiebig, M., Tettich, F., Klaus, C., Franke, H., and Petzold, A.: The IAGOS-CORE aerosol package: instrument design, operation and performance for continuous measurement aboard in-service aircraft, Tellus B, 67, 286-302, 10.3402/tellusb.v67.28339, 2015.

A. Wiedensohler: An approximation of the bipolar charge distribution for particles in the submicron size range, Journal of Aerosol Science, Volume 19, Issue 3, 1988, Pages 387-389, ISSN 0021-8502, doi.org/10.1016/0021-8502(88)90278-9.

Hinds, W. C., Aerosol Technology: Properties, Behavior, and Measurement of Airborne Particles. Wiley: 1999.

Baron, P. A.; Willeke, K., Aerosol measurement: principles, techniques, and applications. 2001.